Preprints.org

Article

Not peer-reviewed version

Enhanced Adsorption Performance Cross-Linked Chitosan/*Citrus reticulata* Peel Waste Composites as Low Cost and Green Bio-Adsorbents: Kinetic, Equilibrium Isotherm, and Thermodynamic Studies

Deniz Akin Sahbaz *

Posted Date: 12 July 2023

doi: 10.20944/preprints202307.0755.v1

Keywords: Citrus reticulata peel waste; chitosan; Congo red; green adsorbents

Preprints.org is a free multidiscipline platform providing preprint service that is dedicated to making early versions of research outputs permanently available and citable. Preprints posted at Preprints.org appear in Web of Science, Crossref, Google Scholar, Scilit, Europe PMC.

Copyright: This is an open access article distributed under the Creative Commons Attribution License which permits unrestricted use, distribution, and reproduction in any medium, provided the original work is properly cited.

Preprints (www.preprints.org) | NOT PEER-REVIEWED | Posted: 12 July 2023 doi:10.20944/preprints202307.0755.v1

Disclaimer/Publisher's Note: The statements, opinions, and data contained in all publications are solely those of the individual author(s) and contributor(s) and not of MDPI and/or the editor(s). MDPI and/or the editor(s) disclaim responsibility for any injury to people or property resulting from any ideas, methods, instructions, or products referred to in the content.

Article

Enhanced Adsorption Performance Cross-Linked Chitosan/*Citrus reticulata* Peel Waste Composites as Low Cost and Green Bio-Adsorbents: Kinetic, Equilibrium Isotherm, and Thermodynamic Studies

Deniz Akin Sahbaz

Department of Chemical Engineering, Faculty of Engineering, Pamukkale University, 20070, Denizli, Turkey; dsahbaz@pau.edu.tr; Tel.: +90 258 296 3094

Abstract: This study revealed the synthesis of cross-linked chitosan/*Citrus reticulata* peel waste (C/CRPW) composites that could be used as low-cost and green bio-adsorbents for the removal of Congo red (CR) dye from aqueous solutions. C/CRPW composites containing different amounts of *Citrus reticulata* peel waste (CRPW) and chitosan were prepared and cross-linked with glutaraldehyde. The composites were characterized by FESEM, FTIR, and BET. The C/CRPW composites as a new type of bio-adsorbents displayed superior adsorption capability toward anionic CR molecules and the adsorption capacities increased by incorporation of CRPW. Effects of different ambient conditions such as contact time, pH, adsorbent dosage, initial adsorbate concentration, and temperature were fully studied. The conditions which obtained 43.57 mg/g of the highest adsorption capacity were conducted at pH 4, initial concentration of 100 mg/L, adsorbent dosage of 2.0 g/L, and contact time of 24 hours at 328 K. The adsorption data was found to follow the pseudo-second-order kinetic model and the Freundlich isotherm model. According to the findings of this investigation, it was observed that the C/CRWP composites can be used as adsorbents due to their advantages of simple preparation process, environmentally friendly, renewable, efficient, and low-cost.

Keywords: *Citrus reticulata* peel waste; chitosan; Congo red; green adsorbents

1. Introduction

Dye pollution in the aquatic water system is a serious environmental problem because of the decrease in photosynthetic activity of water streams and causing disruption of equilibrium of the aquatic environment. Most synthetic dyes found in many industrial wastewater effluents are also toxic and carcinogenic to both human and animal health at a very low percentage of concentration. Various physical, physicochemical, chemical, and biological treatment processes have been used to remove dyes from wastewater, including adsorption [1], membrane separation [2], coagulation–flocculation [3], ion exchange [4], ozonation [5]. Among these techniques, the adsorption has superior advantages such as low investment and operational cost, simple design, easy operation, high effectiveness, and so on for removing dyes.

Congo red (CR) [1-naphthalenesulfonic acid, 3,3′-(4,4′-biphenylenebis (azo)) bis(4-amino-) disodium salt] is an anionic diazo dye [6], used in several industries such as paper, plastic, leather, textiles etc., for colouring their final products. Wastewater containing CR dye is a kind of threatening wastewater because of the difficulty of its degradation. In addition, a carcinogen product such as benzidine is formed as a result of its decomposition under anaerobic conditions [7]. In this present study, CR is chosen as an anionic dye for the adsorption process due to its chemical structure, environmental concern, and potential toxicity to humans. Many adsorbents such as carbonized leonardite [8], nickel-based materials [7], MIL-88A [9], MXene/carbon foam hybrid aerogel [10], polycrystalline α-Fe_2O_3 nanoparticles [11] have been reported in literature for the adsorption of CR

© 2023 by the author(s). Distributed under a Creative Commons CC BY license.

Preprints (www.preprints.org) | NOT PEER-REVIEWED | Posted: 12 July 2023 doi:10.20944/preprints202307.0755.v1

dye. However, most of the commercial adsorbents used in the treatment of dye effluent are not economically viable, some are not technically efficient.

Agricultural waste materials have attracted more attention to be used as adsorbent for the removal of contaminants in aqueous solutions due to their viable properties such as eco-friendly, renewable, and biodegradable nature, inexpensive, availability in abundance, and easy to obtain composites with them. Furthermore, agricultural wastes have various functional groups, which enhance their chemical reactivity and are responsible for removal of various water pollutants. A number of researchers have studied the feasibility of using agricultural solid waste like coir pith [12], potato plant [13], durian peel [14], grape fruit peel [15], mandarin orange peels [16], citrus limetta peel [17], orange peel [18], kiwi peel [19] etc., as adsorbents for the removal of dyes and/or heavy metals from wastewater.

Mandarin (*Citrus reticulata*) peel waste, an agricultural waste from peels that accounts for approximately 30% of the mass of mandarin fruit, is obtained as by-products from the food industry and juice companies, besides household waste [20]. It is estimated that around 110-120 million tons of citrus waste are produced annually worldwide. Dumping of this waste on landfills or marine environments results in nitrogen deficiency during microorganic activities and a significant increase in the levels of biological oxygen demand and chemical oxygen demand [21]. Hence, the reusability of this waste in different areas is significant due to increased environmental damage. The *Citrus reticulata* peel waste (CRPW), abundantly available in Mediterranean countries, Brazil, Japan, Argentina, United States, and Australia, can be used as an effective adsorbent for the removal and recovery of dyes and heavy metals from wastewater because of the various functional groups such as hydroxyl, carboxyl, phenolic, and amino [22]. In this study, CRPW was utilized as an alternative material which offers a high affinity for dye molecules to synthesize polymeric composites as bio-adsorbents.

Chitosan, which has been obtained from alkaline hydrolysis of chitin, is one of the most popular adsorbents for various adsorption processes due to its high absorptivity and affinity for environmental contaminants, biodegradability, biocompatibility, nontoxicity, hydrophilicity, physicochemical characteristics, high chemical reactivity, hydrophilicity [23]. Because of its significant advantages, chitosan has positive feedback from many researchers employing chitosan as an adsorbent. However, chitosan has disadvantages such as poor mechanical strength, thermal instability, and low surface area. In recent studies, it has been observed that this problem has been largely overcome with the use of chitosan-based composites obtained using agricultural waste [24]. However, the literature studies reveal that so far no considerable effort has been made to study the removal of CR dye by chitosan-based composites containing fruit peel of mandarin. In this research, the efficiency of the cross-linked chitosan/*Citrus reticulata* peel waste (C/CRPW) composites in adsorption of CR dye from aqueous solution has been investigated.

Batch experiments were carried out to study the effect of several experimental parameters such as contact time, pH, adsorbent dosage, initial CR concentration, and temperature. Langmuir, Freundlich, Temkin and Dubinin–Radushkevich isotherm models were used to analyse mechanisms of adsorption. The adsorption kinetics was analysed by Lagergren's pseudo-first-order, pseudo-second-order and Weber-Morris intra-particle diffusion kinetic models. Furthermore, the thermodynamic parameters, such as enthalpy, entropy, and free energy, were also investigated. This study explores the possibility of utilizing CRPW to synthesize cross-linked chitosan-based composites as cost-effective and efficient adsorbents for the adsorptive removal of CR dye from polluted wastewater.

2. Materials and Methods

2.1. Materials

Chitosan (Medium Molecular Weight, viscosity 200-800 cP, 1 wt. % in 1% acetic acid, Deacetylation 75-85%) and CR (3,3'-[(1,1'-Biphenyl)-4,4'-diylbis(azo)] bis(4-amino-1-naphthalenesulfonic Acid) 2Na, dye content 97%, CAS 573-58-0) were obtained from Sigma-Aldrich.

Preprints (www.preprints.org) | NOT PEER-REVIEWED | Posted: 12 July 2023 doi:10.20944/preprints202307.0755.v1

Glutaraldehyde (50 wt. % solution in ethanol) was supplied from Acros Organics. Hydrochloric acid (HCl, 37%) and sodium hydroxide (NaOH, reagent grade) were purchased from JT Baker (USA). All materials reached analytical grade and were used directly.

The CRPW used in this study was obtained from the Seferihisar region of Izmir, Turkey. The CRPW was washed with distilled water and cut into 1 cm^2 pieces before dried in an air oven (Natural Convection Oven, JSON-100, JSR Korea) at 100 °C. After drying, it was ground into fine powder and then passed through a sieve to be of size range from 500 μm to 250 μm.

2.2. Preparation of the cross-linked C/CRPW composites

The synthesis processes of cross-linked C/CRPW composites were accomplished based on three main steps. First, the determined amounts of chitosan (1.75 g, 1.50 g, and 1.25 g) were dissolved in 75 mL of acetic acid solutions (5%, w/w) forming gels and then mixed with the different amount of CRPW (0.25 g, 0.50 g, and 0.75 g) under stirring by a magnetic stirrer (Isolab Laborgerate GmbH, Germany) for 24 h. This is followed by treating of C/CRPW powder mixtures by ultrasonic irradiation at 20 kHz, 50% amplitude and no pulsation ultrasound regime at 20 minutes in an ultrasonicator device (Bandelin, HD4100, Germany) to accelerate the intercalation of chitosan between CRPW. The mixtures were then added into the NaOH solutions (1.0 M) dropwise to allow the formation of gel beads and the mixtures were stirred at 150 rpm for another 24 hours. After this process, the obtained C/CRPW composites containing different amounts of chitosan and CRWP were filtered and washed multiple times with deionised water until the pH reached 7. In the third stage, the obtained composites were crosslinked with glutaraldehyde solution (2.5 %, v/v) in a water bath at 60 °C for 24 h to enhance their mechanical properties and stability in acidic solutions. Lastly, dried C/CRPW composites were obtained by washing these composites exhaustively with deionised water three times followed by drying in an oven (Natural Convection Oven, JSON-100, JSR Korea) at 60 °C for 48 h.

The cross-linked C/CRPW composites containing different amounts of chitosan and CRPW were referred to as xC/yCRPW, where x and y denote the amount of chitosan and CRPW used in the synthesis process, respectively. Three different composites obtained in this study were named 1.75C/0.25CRPW, 1.50C/0.50CRPW and 1.25C/0.75CRPW.

2.3. Characterization of the cross-linked C/CRPW composites

The field emission scanning electron microscope (FESEM, Gemini Supra 40 VP, Zeiss, Germany) was used to determine the surface morphology of the cross-lined C/CRPW composites at 10.00 kV. The composites were coated with a thin layer of gold using a sputter coater. The chemical structure of the cross-linked C/CRPW composites was determined by using a Fourier transfer infrared (FTIR) spectroscope (Thermo Scientific Nicolet iS50FT-IR). The spectral data of all composites were acquired in the wavenumber range of 400–4000 cm^{-1} with 50 scans at a resolution of 4 cm^{-1}. N_2 adsorption-desorption was measured at liquid nitrogen temperature 77 K using a Quantachrome Autosorb-1C-MS instrument. The specific surface area was determined by the multipoint Brunauer-Emmett-Teller (BET) technique. The pore volume and pore size were derived from the desorption branches of the isotherms using the Barrett–Joyner–Halenda (BJH) method.

2.4. Batch adsorption studies

The adsorption of CR dye onto the C/CRPW composites (1.75C/0.25CRPW, 1.50C/0.50CRPW, and 1.25C/0.75CRPW) was carried out in batch mode. A stock solution of CR dye (1000 mg/L) was prepared, which was diluted to desired concentrations for further usage. All the adsorption experiments were performed by adding the determined amount of adsorbent to 100 mL CR dye solutions in a thermostatic shaker bath (Nuve ST 30) at a fixed agitation speed of 150 rpm for the pre-determined time. The pH of CR dye solutions was adjusted using HCl (0.1 N) and NaOH (0.1 N) solutions. After adsorption, the concentration of CR dye was measured spectrophotometrically by

Preprints (www.preprints.org) | NOT PEER-REVIEWED | Posted: 12 July 2023 doi:10.20944/preprints202307.0755.v1

monitoring the absorbance at 497 nm using a Hitachi U-2900 spectrophotometer (Hitachi High Technologies Corporation, Tokyo, Japan).

The equilibrium adsorption capacities of the C/CRPW composites (q_e (mg/g)) were estimated using Equation (1):

$$q_e = \frac{C_i - C_e}{m} \times V \quad (1)$$

where C_i is the initial dye concentration (mg/L), C_e is the dye concentration at equilibrium (mg/L), V is the volume of dye solution (L), and m is the mass of the adsorbents (g).

Effects of contact time (0-24 hours), initial solution pH (4-9), adsorbent dosage (2-6 g/L), initial CR concentration (20-100 mg/L), and temperature (298.15-328.15 K) on the adsorption of CR dye were investigated. To verify that the results are repeatable, all adsorption experiments were conducted in triplicates and the mean value reported.

3. Results

3.1. Characterization of the cross-linked C/CRPW composites

The FESEM images of 1.75C/0.25CRPW, 1.50C/0.50CRPW, and 1.25C/0.75CRPW composites are presented in Figure 1. As shown in Figure 1, all the composites have broadly large pores, while many pores of different sizes are observed. The 1.25C/0.75CRPW composites have rougher surfaces, more porous with well-developed pore openings, and more irregular shapes than the other composites. The surface roughness of the adsorbents affects the adsorption capacity as it causes high hydrophilicity [25].

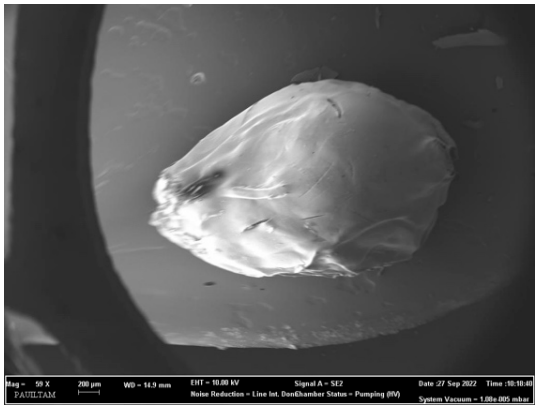

(**a**)

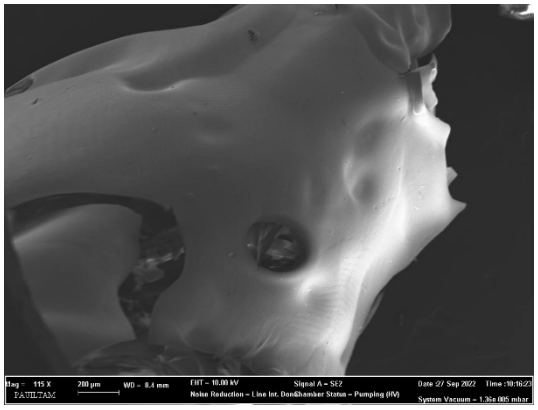

(**b**)

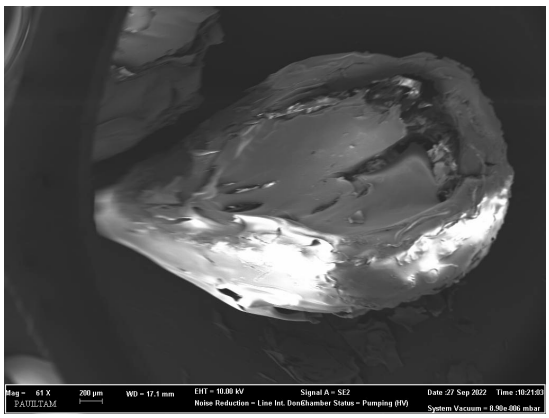

(**c**)

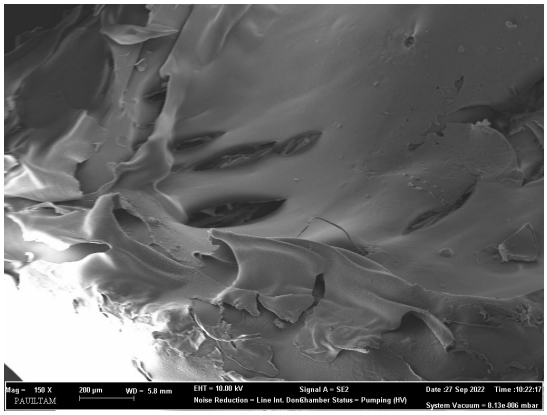

(**d**)

Preprints (www.preprints.org) | NOT PEER-REVIEWED | Posted: 12 July 2023 doi:10.20944/preprints202307.0755.v1

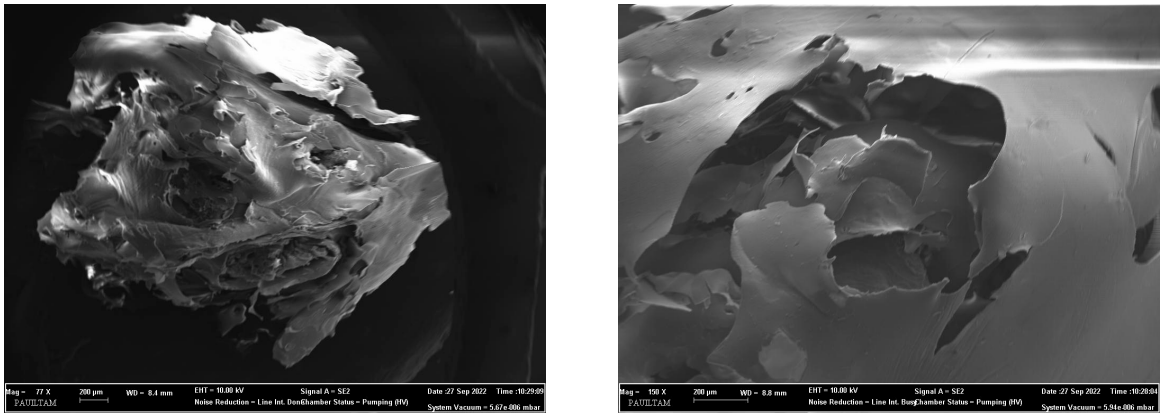

(e) **(f)**

Figure 1. FESEM images of the cross-linked 1.75C/0.25CRPW (a,b), 1.50C/0.50CRPW (c,d), and 1.25C/0.75CRPW composites (e,f).

The FTIR spectra of C, CRPW, and the cross-linked C/CRPW composites are given in Figure 2. The FTIR spectrum of CRPW showed the broad and intense band at 3286 cm^{-1} corresponding to the O–H stretching vibration that existed in the inter and intramolecular hydrogen bonding [26]. The bands at 2920 and 1734 cm^{-1} can be attributed to the C–H stretching and C=O stretching vibrations of carboxy groups appearing in CRPW constituents such as pectin, lignin, and cellulose [27]. The C-H group band at 2920 cm^{-1} of CRPW was moved to around 2930 cm^{-1} in the cross-linked C/CRPW composites, while the C=O group observed at 1734 cm^{-1} of CRPW was moved to 1653 cm^{-1} in the cross-linked C/CRPW composites. Decreased intensity and shifting of these peaks could be a result of a lower cellulose content in the cross-linked C/CRPW composites. Furthermore, the strong band at 1016 cm^{-1} represents the C–O–H functional group in CRPW, while it is observed in the cross-linked C/CRPW composites at around 1027 cm^{-1} [16].

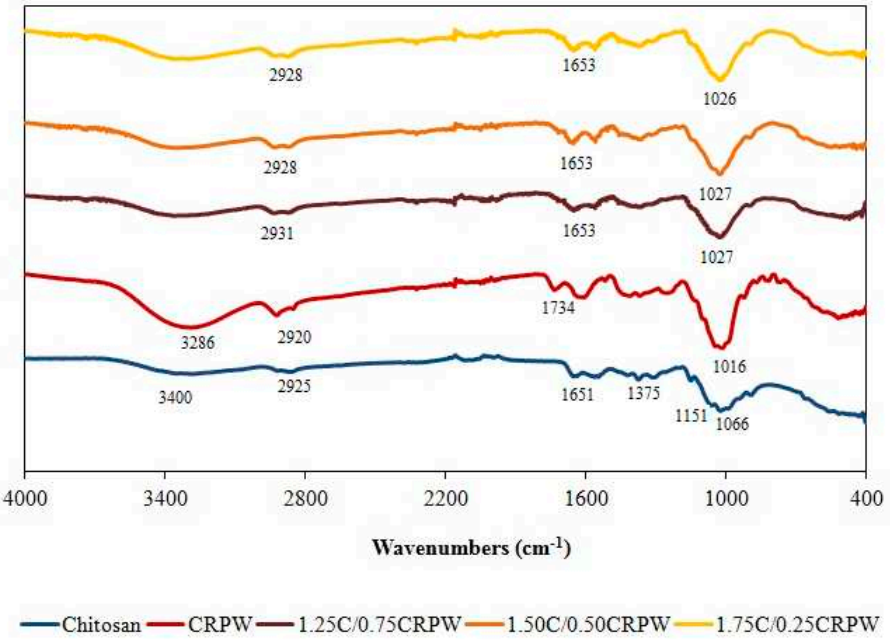

Figure 2. FTIR spectra of chitosan, CRPW, and the cross-linked C/CRPW composites.

The FTIR spectrum of chitosan showed main peaks at 3400, 2925, 1651, 1375, 1151, and 1066 cm^{-1}, representing the N–H and O–H stretching vibration, CH_3 symmetric stretch, C=O stretching vibration, CH_3 bending vibration, C–O–C bending vibration, and C–OH stretching vibration,

Preprints (www.preprints.org) | NOT PEER-REVIEWED | Posted: 12 July 2023 doi:10.20944/preprints202307.0755.v1

respectively. The peaks observed at 1375 cm^{-1} and 1151 cm^{-1} in the FTIR spectrum of chitosan disappeared in the FTIR spectrum of the cross-linked C/CRPW composites because of cross-linking of chitosan with glutaraldehyde. Besides, the spectrum of the cross-linked C/CRPW composites shows a new peak at 1650 cm^{-1} that can be attributed to amide (-C(=O)N-) due to the cross-linking reaction of chitosan and glutaraldehyde [28].

A nitrogen isothermal adsorption technique was employed to investigate the textural properties and pore structure of the CRPW and cross-linked C/CRPW composites. BET specific surface area, average pore diameter and total pore volume based on BJH theory of the sample were measured and represented in Table 1. It has been found that the increase in CRPW amount in chitosan matrix leads to an increase in surface area and total pore volume of the C/CRPW composites. This result explains that the interfacial interaction between the chitosan matrix and CRPW greatly affects the material pore structure [29].

Table 1. Surface parameters of the CRPW and cross-linked C/CRPW composites.

Samples	BET surface area (m^2/g)	BJH pore volume (cm^3/g)	BJH pore size (A°)
1.75C/0.25CRPW	10.04	0.06225	29.83
1.50C/0.50CRPW	13.86	0.1014	16.17
1.25C/0.75CRPW	20.42	0.1500	16.39
CRPW	17.61	0.02269	18.85

3.2. Effect of contact time and adsorption kinetic models

The effect of contact time on the adsorption capacities of the 1.75C/0.25CRPW, 1.50C/0.50CRPW, and 1.25C/0.75CRPW composites is shown in Figure 3a. As shown in Figure 3a), adsorption capacity increases with contact time and reaches equilibrium after 24 hours. However, the increase in adsorption capacity values is relatively higher during the initial 12 hours due to the plenty of vacant sites available for the adsorption of CR molecules. Consequently, a large mass transfer rate was observed during the initial 12 hours of the process and equilibrium was achieved at approximately 95% efficiency. After that, a gradual decrease in the adsorption rate is observed until 24 hours as the empty spaces on the adsorbent surface gradually decrease. After 24 hours, equilibrium was achieved for all the cross-linked C/CRPW composites.

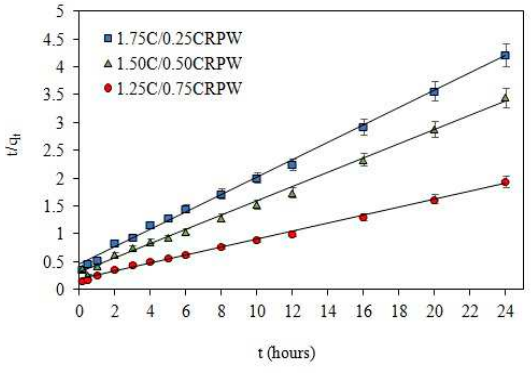

(**a**)

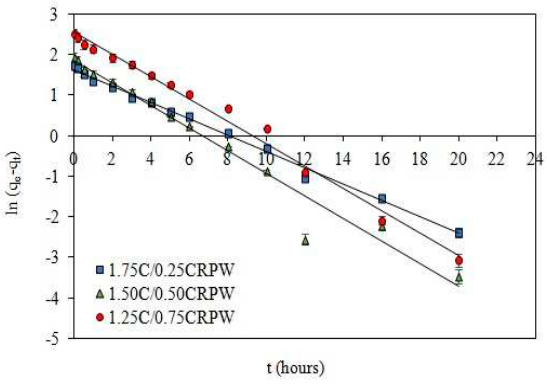

(**b**)

Preprints (www.preprints.org) | NOT PEER-REVIEWED | Posted: 12 July 2023 doi:10.20944/preprints202307.0755.v1

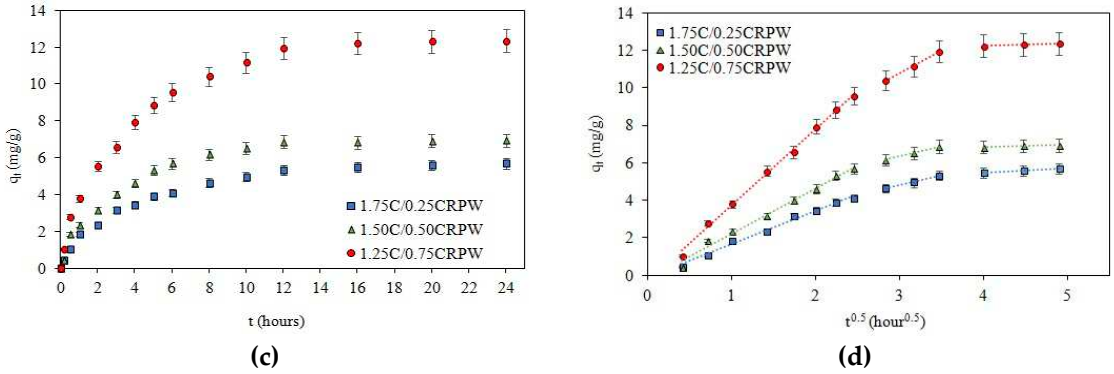

(c) (d)

Figure 3. Adsorption amount of CR onto the cross-linked C/CRPW composites varying with time (a) and linear fitting of Lagergren's pseudo-first-order (b), pseudo-second-order (c), intra-particle diffusion (d) (experimental conditions: adsorbent dosage = 2 g/L; initial dye concentration = 60 mg/L; pH = 7; temperature = 298 K).

The Lagergren's pseudo-first-order and the pseudo-second-order kinetic models were used to evaluate the adsorption kinetics of CR onto the cross-linked C/CRPW composites.

Lagergren's pseudo-first-order kinetic model [30]:

$$\ln(q_e - q_t) = \ln q_e - k_1 . t \quad (2)$$

Pseudo-second-order kinetic model [31]:

$$\frac{t}{q_t} = \frac{1}{k_2 . q_e^2} + \frac{t}{q_e} \quad (3)$$

where q_e and q_t (mg/g) are the adsorption amount of CR at equilibrium and t (hour), respectively; k_1 (1/hour) and k_2 (g/mg hour) are the rate constants of the Lagergren's pseudo-first-order and pseudo-second-order model, respectively.

The representative graphs for Lagergren's pseudo-first-order and pseudo-second order equations are displayed in Figure 3b and Figure 3c, respectively, and the kinetic model parameters are shown in Table 2.

It can be seen from the data in Table 2, the pseudo-second-order model has a higher correlation coefficient (R^2>0.99) for CR adsorption onto all the cross-linked C/CRPW composites. It was observed that the adsorption capacities of 1.75C/0.25CRPW and 1.50C/0.50CRPW composites were not very different from each other. The adsorption capacities of 1.75C/0.25CRPW and 1.50C/0.50CRPW were 5.69 mg/g and 6.94 mg/g, respectively. The data also showed that the adsorption capacity of the C/CRPW composites increases with increasing CRPW contents. The 1.25C/0.75CRPW composites exhibited the best adsorption performance among the composites. This result might be due to the addition of CRPW increasing the specific surface area. This result is supported by SEM images shown in Figure 1.

The Weber-Morris intra-particle diffusion model was also studied to better understand the adsorption mechanism of CR dye onto the cross-linked C/CRPW composites.

Equation (4) shows the linear form of the intra-particular diffusion kinetic model [32]:

$$q_t = C + K_{id} . t^{0.5} \quad (4)$$

where q_t is the adsorption amount of CR at t (hour), t is adsorption time (hour), K_{id} (mg/g hour$^{0.5}$) is intra-particle diffusion rate constant, and C is mass transfer residence due to the thickness of the boundary layer.

The intra-particle diffusion plots of adsorption capacity qt versus $t^{0.5}$ for the adsorption of CR onto the cross-linked C/CRPW composites are shown in Figure 3d. The kinetic parameters, K_{id} and C, were determined by the intercept and slope of linear plots and given in Table 2. As can be seen from Figure 3d, the linear lines at early contact times did not pass through the origin, suggesting that there was a boundary layer effect and internal diffusion was not merely a rate-controlling step. In other

Preprints (www.preprints.org) | NOT PEER-REVIEWED | Posted: 12 July 2023 doi:10.20944/preprints202307.0755.v1

words, the adsorption of the CR molecules onto the cross-linked C/CRPW composites was controlled by more than one adsorption rate process. The phenomena can be explained by the presence of micropores in the cross-linked C/CRPW composites [33].

Table 2. Kinetic parameters of the Lagergren's pseudo-first-order, pseudo-second-order, and intra-particle diffusion kinetic models for CR onto the cross-linked C/CRPW composites.

Models	Parameters	Values		
		1.75C/0.25CRPW	1.50C/0.50CRPW	1.25C/0.75CRPW
Experimental result	$q_{e,exp}$ (mg/g)	5.69	6.94	12.35
Lagergren's pseudo-first-order	$q_{e,cal}$ (mg/g)	5.09	6.34	12.81
	k_1 (1/hour)	0.2021	0.2775	0.2763
	R^2	0.9950	0.9652	0.9893
Pseudo-second-order	$q_{e,cal}$ (mg/g)	6.39	7.78	13.91
	k_2 (g/mg hour)	0.0545	0.0548	0.0275
	R^2	0.9971	0.9963	0.9968
Intra-particle diffusion	$k_{id,1}$ (mg/g hour$^{0.5}$)	1.7985	2.4436	4.0972
	C_1	-0.1430	-0.2177	-0.3548
	R^2	0.9901	0.9876	0.9968
	$k_{id,2}$ (mg/g hour$^{0.5}$)	1.0920	1.0936	2.4286
	C^2	1.5399	3.0752	3.5203
	R^2	0.9954	0.9997	0.9984
	kid,3 (mg/g hour$^{0.5}$)	0.2411	0.1211	0.1380
	C_3	4.5149	6.3582	11.682
	R^2	0.9972	0.9551	0.9870

Three distinct stages for the adsorption of CR onto the cross-linked 0.25W/1.75CRPW, 0.50W/1.50CRPW, and 0.75W/1.25CRPW composites were identified from the fitting of Equation 4. The stages were 0–6 hours, 8–12 hours, and 16–24 hours, representing the first, second, and third stages, respectively. During the first stage, at the beginning of the process, the adsorption speed was faster and diffusion of CR molecules from the solution to the external surface of cross-linked C/CRPW composites played an essential role, which was related to external diffusion. In the second stage, a slower adsorption rate was observed, referring to intra-particle diffusion (internal diffusion). Afterwards, in the third stage, which acquired a kinetic balance, the equilibrium of adsorption and desorption was observed [19]. In addition, as shown in Table 2, the diffusion rate constant values in the first and second stage for 1.25C/0.75CRPW composites were higher than those for 1.50C/0.50CRPW and 1.75C/0.25CRPW composites. The higher Kid value, the easier diffusion and transport into the pores of adsorbents are [34]. According to these results, the increasing amount of CRPW in the composition of composites causes the increasing diffusion and transportation of CR molecules into the interior of the composites.

3.3. Effect of initial solution pH

The initial solution pH is a significant parameter in adsorption processes because it influences the chemistry of both the adsorbate and the adsorbents. CR is a pH-sensitive dye, resulting in the dye changing colour from red to blue. The original pH of the CR solution is around 7.0. The adsorption of CR on the cross-linked C/CRPW composites was studied in the pH range 4–9, in which range the colour of CR is stable and red. Figure 4a shows the effect of initial solution pH on the adsorption of CR by the 1.75C/0.25CRPW, 1.50C/0.50CRPW, and 1.25C/0.75CRPW composites. As shown in Figure 4a, there was a decrease in adsorptive capacity of all the composites with increasing initial solution

Preprints (www.preprints.org) | NOT PEER-REVIEWED | Posted: 12 July 2023 doi:10.20944/preprints202307.0755.v1

pH, indicating that the adsorption of CR by the composites was pH dependent. The highest adsorptive capacity for all the composites (1.75C/0.25CRPW 19.63 mg/g; 1.50C/0.50CRPW 20.41 mg/g; 1.25C/0.75CRPW 23.48 mg/g) was obtained at the lowest pH of 4. The reason for this result is that at higher pH values, the anionic ions from the CR compete with the more hydroxyl ions in the adsorption solution. Similar results have been reported by other researchers [35-36].

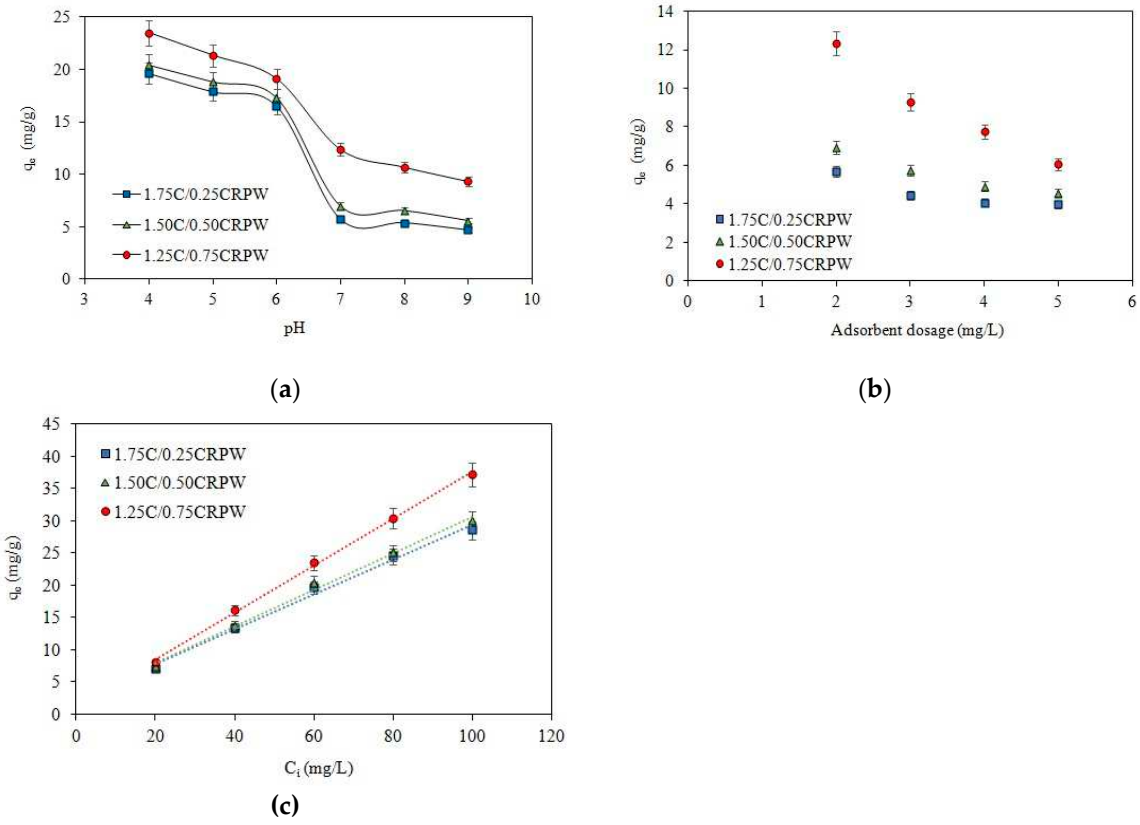

Figure 4. Effect of initial solution pH (a), adsorbent dosage (b), and initial dye concentration (c) on the adsorption of CR onto the cross-linked 1.75C/0.25CRPW, 1.50C/0.50CRPW, and 1.25C/0.75CRPW composites (experimental conditions: adsorbent dosage = 2 g/L; contact time = 24 hours; initial dye concentration = 60 mg/L; temperature = 298 K).

3.4. Effect of adsorbent dosage

Adsorbent dosage is a crucial factor in the adsorption process due to impacts on both the process cost and the removal percentage of contaminants. The effect of the adsorbent dosage on the CR adsorption on 1.75C/0.25CRPW, 1.50C/0.50CRPW, and 1.25C/0.75CRPW composites was examined by increasing adsorbent dosage from 2 to 6 g/L at constant experimental conditions, and the results are shown in Figure 4b. As increasing the adsorbent dosage, more adsorption sites are available for CR dye molecules resulting in reduction of the adsorption capacity of adsorbents. As seen in Figure 4b, as the adsorbent dosage increased from 2 to 6 g/L, the adsorption capacity decreased from 3.98 to 5.69 mg/g, 4.58 to 6.94 mg/g, and 6.07 to 12.35 mg/g for the 1.75C/0.25CRPW, 1.50C/0.50CRPW, and 1.25C/0.75CRPW composites, respectively. 2 g/L of adsorbent dosage was selected as an optimum dosage for further experiments due to more active sites of the composites remaining unsaturated during the CR dye adsorption process.

3.5. Effect of initial CR concentration

The effect of the initial CR dye concentration on the adsorption capacities of the 1.75C/0.25CRPW, 1.50C/0.50CRPW, and 1.25C/0.75CRPW composites was investigated by changing dye concentration from 20 to 100 mg/L at constant experimental conditions. As shown in Figure 4c,

Preprints (www.preprints.org) | NOT PEER-REVIEWED | Posted: 12 July 2023 doi:10.20944/preprints202307.0755.v1

when the initial dye concentration was increased to 20 and 100 mg/L, the adsorption capacities of 1.75C/0.25CRPW, 1.50C/0.50CRPW, and 1.25C/0.75CRPW composites increased from 7.10 to 28.52 mg/g, 7.31 to 30.00 mg/g, and 8.06 to 37.21 mg/g, respectively. The adsorption capacities of all the composites were improved by increasing the CR dye concentration in the aqueous solution due to the higher collision probability between active sites of the composites and the CR dye molecules [37].

3.6. Adsorption isotherms

The nature of the adsorption process of CR onto the 1.75C/0.25CRPW, 1.50C/0.50CRPW, and 1.25C/0.75CRPW composites was examined with Langmuir [38], Freundlich [39-40], Temkin [41], and Dubinin–Radushkevich [42] isotherm models. The linear forms of these isotherm models can be expressed as:

Langmuir

$$\frac{C_e}{q_e} = \frac{C_e}{q_{max,L}} + \frac{1}{K_L q_{max,L}} \quad (5)$$

Freundlich

$$\ln q_e = \ln K_F + (1/n) \ln C_e \quad (6)$$

Temkin

$$q_e = B_T \ln K_T + B_T . \ln C_e \quad (7)$$

Dubinin–Radushkevich

$$\ln q_e = \ln q_{max,D-R} - K_{D-R} . \varepsilon^2 \quad (8)$$

where K_L is the Langmuir equilibrium constant (L/mg) and used to calculate equilibrium dimensionless parameter (R_L), which is defined by $R_L = 1/(1 + K_L . C_i)$ and determines the feasibility of the Langmuir model, $q_{max,L}$ is the Langmuir maximum monolayer adsorption capacity (mg/g), K_F is the Freundlich constant also known as adsorption capacity ((mg/g)(mg/L)$^{-1/n}$) which describes the adsorption capacity, $1/n$ is the Freundlich intensity parameter representing surface heterogeneity, K_T is the Temkin isotherm equilibrium binding constant (L/mg), B_T is Temkin constant i.e. heat of adsorption (J/mol), $q_{max,D-R}$ is the Dubinin–Radushkevich maximum adsorption capacity (mg/g), K_{D-R} is a constant related to sorption energy (mol^2/kJ^2), and ε is the Polanyi potential (kJ/mol).

The ε value can be calculated using Equation (9):

$$\varepsilon = R . T . \ln\left(\frac{C_e + 1}{C_e}\right) \quad (9)$$

where R of 8.314 J/mol.K is the universal gas constant and T is the absolute temperature in Kelvin.

The mean free energy of adsorption (E, kJ/mol) can be calculated using Equation (10):

$$E = \frac{1}{\sqrt{2K_{D-R}}} \quad (10)$$

The free energy can determine the type of adsorption process. If E is less than 8 kJ/mol the adsorption process is physisorption, while if it is more than 8 kJ/mol the process is chemisorption.

The linear fitting for the Langmuir, Freundlich, Temkin, and Dubinin–Radushkevich isotherms is shown in Figure 5, and the calculated isotherm parameters are listed in Table 3.

Preprints (www.preprints.org) | NOT PEER-REVIEWED | Posted: 12 July 2023 doi:10.20944/preprints202307.0755.v1

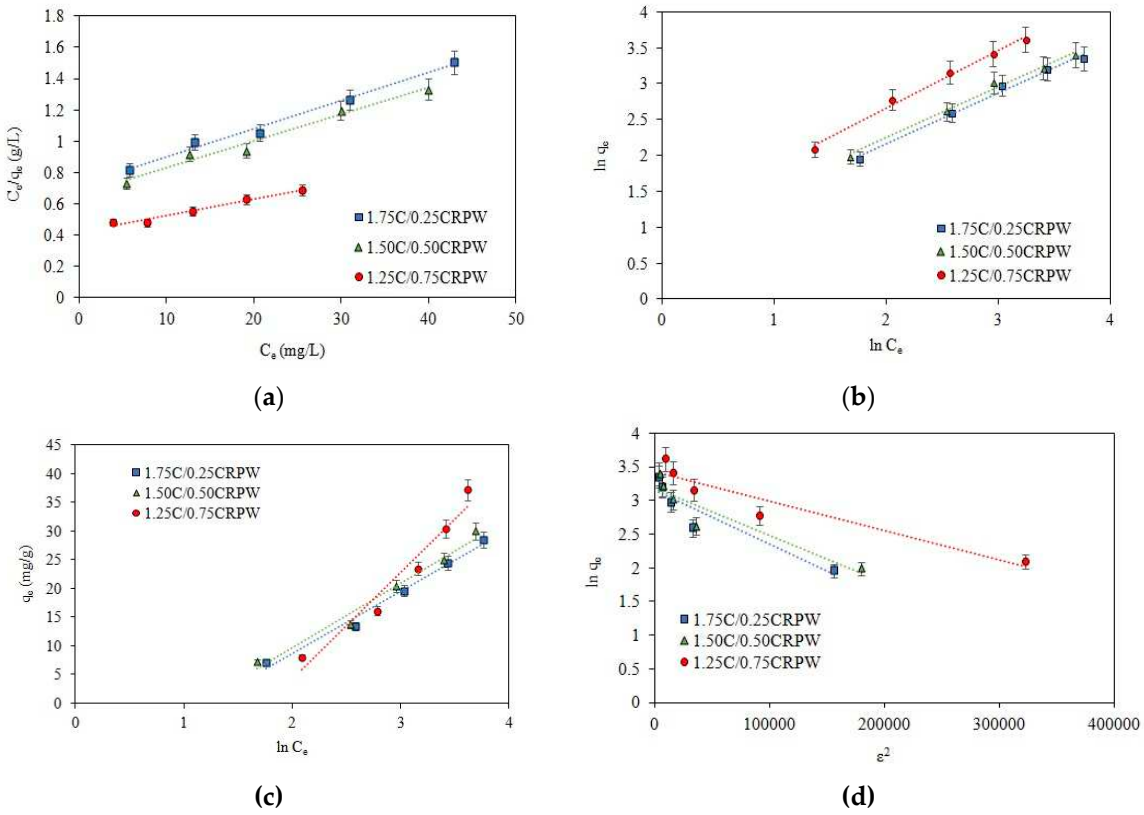

Figure 5. Langmuir (a), Freundlich (b), Temkin (c), and Dubinin–Radushkevich (d) adsorption isotherm models of CR onto the cross-linked 1.75C/0.25CRPW, 1.50C/0.50CRPW, and 1.25C/0.75CRPW composites (experimental conditions: adsorbent dosage = 2 g/L; contact time = 24 hours; pH =4; temperature = 298 K).

The values of correlation coefficient R^2 were used to determine the suitable isotherms, which explain the adsorption process. In this study, the Freundlich isotherm model was best fitted for all the cross-linked C/CRPW composites with R^2 values of 0.9904–0.9908. Hence, it can thus be concluded that the adsorption process takes place on a heterogeneous surface of the composites. When the K_F values of the cross-linked C/CRPW composites are compared, it was observed to increase of K_F values from 2.115–2.886 as the amount of CRPW in the composite contents was increased from 0.25 g to 0.75 g which confirmed the above kinetic and equilibrium studies where dye adsorption capacity increased as CRPW contents in the composites was raised.

The maximum adsorption capacities of the 1.75C/0.25CRPW, 1.50C/0.50CRPW, and 1.25C/0.75CRPW composites were calculated using the Langmuir isotherm equation (Equation 5) to adsorb CR was found to 55.56 mg/g, 58.48 mg/g, and 97.09 mg/g, respectively. Although the R^2 values of the Langmuir isotherm model (R^2 = 0.9714–0.9895) were low, the calculated R_L values (0.2779-0.6729) as shown in Table 3 were found to be between zero and one, indicating that the adsorption was a favourable process.

Table 3. Adsorption isotherm parameters for adsorption of CR onto the cross-linked C/CRPW composites.

Isotherm	Constants	1.75C/0.25CRPW	1.50C/0.50CRPW	1.25C/0.75CRPW
Langmuir	$q_{max,L}$ (mg/g)	55.56	58.48	97.09
	K_L (L/mg)	0.0251	0.0260	0.0243
	R_L	0.6659-0.2851	0.6581-0.2779	0.6729-0.2915
	R^2	0.9895	0.9764	0.9714
Freundlich	n	1.4102	1.4098	1.2472

Preprints (www.preprints.org) | NOT PEER-REVIEWED | Posted: 12 July 2023 doi:10.20944/preprints202307.0755.v1

	K_F ((mg/g)(mg/L)$^{-1/n}$)	2.115	2.284	2.886
	R^2	0.9904	0.9907	0.9908
Temkin	B_T (J/mol)	10.88	11.28	18.56
	K_T (L/mg)	0.3003	0.3193	0.1706
	R^2	0.9844	0.9771	0.9520
Dubinin-Radushkevich	$q_{max,D\text{-}R}$ (mg/g)	23.50	24.23	30.66
	$K_{D\text{-}R}$ (mol^2/J^2)	8 x 10-6	7 x 10-6	4 x 10-6
	E (kJ/mol)	0.250	0.267	0.353
	R^2	0.8736	0.8631	0.9049

The heat of adsorption (B_T) of all the composites calculated from the Temkin isotherm model was found to increase from 10.88 to 18.56 (J/mol) as the amount of CRPW was raised in the structure of the cross-linked C/CRPW composite. The relatively high correlation coefficient values (R^2 = 0.9520–0.9844) of the Temkin model for all cross-linked C/CRPW composites showed the suitability of the model in interpreting the adsorption process. The values of E (0.250-0.353 kJ/mol) calculated from the Dubinin–Radushkevich isotherm model using Equation (10) were found to be < 8 kJ/mol, indicating that the physisorption plays a dominant role in adsorption of CR dye onto all the cross-linked C/CRPW composites [43]. The low correlation coefficient (R^2 = 0.8631–0.9049) of the Dubinin–Radushkevich model indicated the weakness of the model in clarifying the adsorption process.

3.7. Effect of temperature and adsorption thermodynamics

Thermodynamic studies for the adsorption of CR dye on the 1.75C/0.25CRPW, 1.50C/0.50CRPW, and 1.25C/0.75CRPW composites were carried out within temperature-dependent adsorption in the range of 298–328 K. The temperature effect on the adsorption capacities of all the composites for CR dye indicated that the uptake capacity of CR dye increases with increasing the temperature from 298 K to 328 K, which result in adsorption of CR dye onto the cross-linked C/CRPW composites is endothermic reaction.

Thermodynamic parameters including Gibbs free energy change (ΔG°), enthalpy change (ΔH°), and entropy change (ΔS°) of the adsorption process were calculated using the following equations [44]:

$$\Delta G^\circ = -RT \ln K_C \quad (11)$$

$$K_C = q_e / C_e \quad (12)$$

$$\ln K_C = \frac{\Delta S^\circ}{R} - \frac{\Delta H^\circ}{R.T} \quad (13)$$

where R is the gas constant (8.314 J/mol.K), T is the absolute temperature (K), Kc represents the distribution coefficient.

The values of ΔH° and ΔS° can be determined from the Van't Hoff plot, which is the linear plot of In K_C versus 1/T (Figure 6), from the slope and intercept, respectively. The thermodynamic parameters are presented in Table 4.

The negative values of ΔG° suggest the spontaneity of the adsorption processes. As shown in Table 4, the higher absolute values of ΔG° were observed at higher temperatures for all the cross-linked C/CRPW composites. Thus, the adsorption of CR dye onto the cross-linked C/CRPW composites is more spontaneous and favourable at higher temperatures. However, at lower temperatures, the positive values of ΔG° for the adsorption of CR dye onto the 1.75C/0.25CRPW and 1.50C/0.50CRPW composites indicate the nonspontaneous and unfavourable adsorption process.

Preprints (www.preprints.org) | NOT PEER-REVIEWED | Posted: 12 July 2023 doi:10.20944/preprints202307.0755.v1

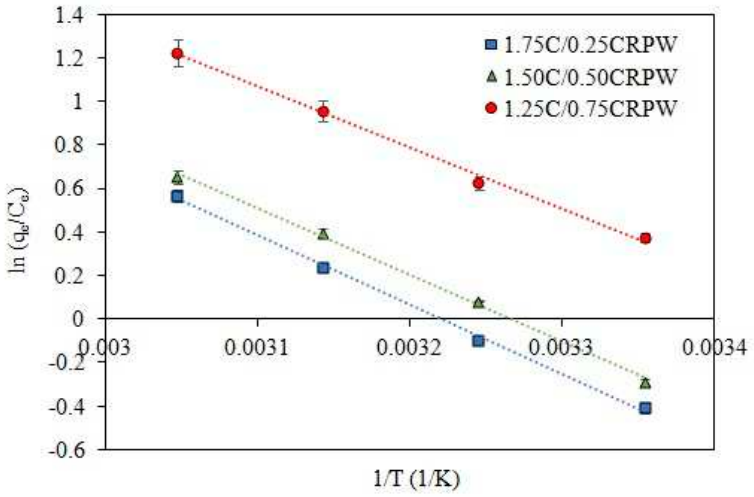

Figure 6. Van't Hoff plot for the adsorption of CR dye onto the cross-linked 1.75C/0.25CRPW, 1.50C/0.50CRPW, and 1.25C/0.75CRPW composites (experimental conditions: adsorbent dosage = 2 g/L; contact time = 24 hours; initial dye concentration = 100 mg/L; pH =4).

The adsorption of CR dye onto the 1.75C/0.25CRPW, 1.50C/0.50CRPW and 1.25C/0.75CRPW composites had enthalpy changes of 26.465, 25.528, and 23.358 kJ/mol, respectively. The positive and lower than 40 kJ/mol of ΔH° values confirm that it is an endothermic process in physical interaction between CR molecules and all the cross-linked C/CRPW composites established. In addition, the positive values of ΔS° suggest an increased randomness at the solid/solution interface during the adsorption of CR dye onto all the cross-linked C/CRPW composites [45].

Table 4. Thermodynamic parameters for the adsorption of CR onto the cross-linked C/CRPW composites.

Thermodynamic parameters	T (K)	1.75C/0.25CRPW	1.50C/0.50CRPW	1.25C/0.75CRPW
ΔG° (J/mol)	298.15	1052.27	668.89	-878.22
	308.15	199.92	-164.92	-1691.12
	318.15	-652.43	-998.73	-2504.01
	328.15	-1504.78	-1832.54	-3316.90
ΔH° (kJ/mol)		26.465	25.528	23.358
ΔS° (J/mol.K)		85.235	83.38	81.29

3.8. Reusability studies

The reusability of 1.75C/0.25CRPW, 1.50C/0.50CRPW, and 1.25C/0.75CRPW composites was investigated by six cycles of adsorption–desorption process and the results were shown in Figure 7. NaOH solution was used in desorption studies to facilitate the diffusion of CR molecules from the active sites of the composites. The recovered composites were washed with deionized water several times and dried for the next adsorption test. As shown in Figure 7, the adsorption capacities of 1.75C/0.25CRPW, 1.50C/0.50CRPW, and 1.25C/0.75CRPW composites for CR gradually decreased with increasing number of cycles. However, after six adsorption-desorption cycles, the 1.75C/0.25CRPW, 1.50C/0.50CRPW, and 1.25C/0.75CRPW composites remained 90.0, 88.7, 87.7% of its initial CR adsorption capabilities, respectively. The high values of q_e value are due to the improved mechanical stability of the composites by cross-linking of chitosan containing CRPW with glutaraldehyde [24]. The recyclability studies reveal that the cross-linked C/CRPW composites as bio-adsorbents in practical applications show high performance and sustainability.

Preprints (www.preprints.org) | NOT PEER-REVIEWED | Posted: 12 July 2023 doi:10.20944/preprints202307.0755.v1

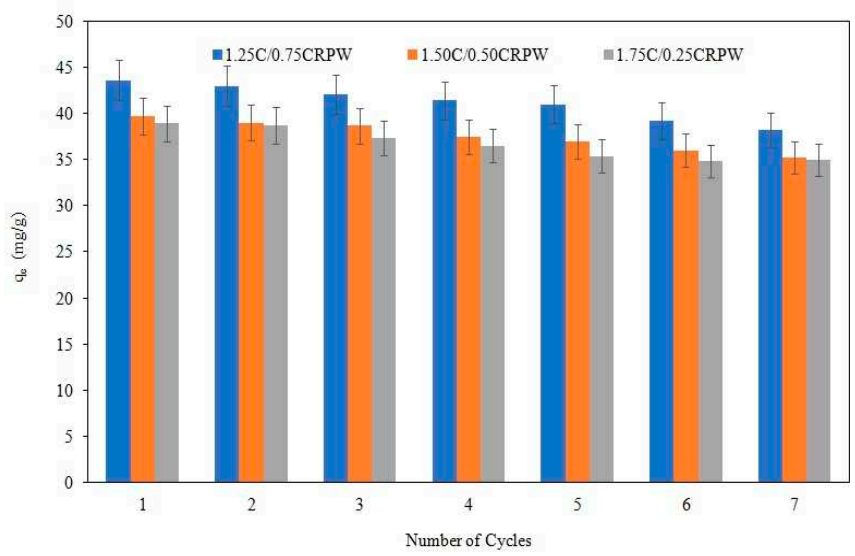

Figure 7. Recycling of the cross-linked 1.75C/0.25CRPW, 1.50C/0.50CRPW, and 1.25C/0.75CRPW composites for the removal of CR.

3.9. Comparative study

The maximum adsorption capacities of 1.75C/0.25CRPW, 1.50C/0.50CRPW, and 1.25C/0.75CRPW composites are found to be 38.92 mg/g, 39.66 mg/g, and 43.57 mg/g, respectively. Table 5 shows the maximum adsorption capacities of different adsorbents obtained by different agricultural waste for CR dye. All the cross-linked C/CRPW composites obtained in this study have a relatively high adsorption capacity, which suggests that they can be preferred to use as an adsorbent for removing CR due to their excellent properties, such as readily available, environment-friendly, and cost-effectiveness.

Table 5. Comparison of maximum adsorption capacities of different adsorbents obtained by different agricultural waste for CR dye.

Adsorbent	Adsorption capacity (mg/g)	References
Cabbage waste powder	2.313	[46]
Activated carbon prepared from coir pith	6.72	[47]
Bengal gram fruit shell	22.22	[48]
Coconut-based activated carbon fibers	22.1	[49]
Chinese yam peel–polypyrrole composites	86.66	[50]
Tunics of the corm of the saffron	6.2	[51]
1.75C/0.25CRPW composites	38.92	Present work
1.50C/0.50CRPW composites	39.66	Present work
1.25C/0.75CRPW composites	43.57	Present work

4. Conclusions

In the present research work, three cross-linked chitosan-based composites containing mandarin (*Citrus reticulata* Seferihisar cv.) peel waste, namely 1.75C/0.25CRPW, 1.50C/0.50CRPW, and 1.25C/0.75CRPW, as new low cost and green adsorbents have been successfully synthesized for removal of the toxic anionic dye, CR, from aqueous solution. 1.25C/0.75CRPW composites performed the best adsorption capacity (43.57 mg/g) for CR removal from aqueous solutions, followed by 1.50C/0.50CRPW composites (39.66 mg/g) and 1.75C/0.25CRPW composites (38.92 mg/g). The results showed that the increase in CRPW content of the cross-linked C/CRPW composites resulted in an

Preprints (www.preprints.org) | NOT PEER-REVIEWED | Posted: 12 July 2023 doi:10.20944/preprints202307.0755.v1

increase of adsorption capacity because of the enhancement of the porosity of the composite surface. The influence of various operating parameters such as contact time, pH, adsorbent dosage, initial dye concentration, and temperature on the adsorption capacities of all the composites was investigated. Compared with the effect of factors on the adsorption capacities of the composites, all parameters influenced the adsorption capacities, but also the effect of pH change on the adsorption capacities was more obvious. The highest adsorption capacity values were obtained in adsorption conditions where pH of 4, adsorbent dosage of 2 g/L, the initial CR dye concentration of 100 mg/L, and adsorption temperature of 328 K. The adsorption kinetics for all the composites investigated in this work followed the pseudo-second-order equation. The adsorption equilibrium data also could be well described by the Freundlich isotherm model. The high adsorption ability of the cross-linked C/CRPW composites and the abundant availability of CRPW as waste material revealed that these composites can be used as low cost and green bio-adsorbents for removal of CR dye in industrial wastewater.

Funding: This research received no external funding.

Data Availability Statement: The data presented in this study are available on request from the corresponding author.

Acknowledgments: The authors wish to thank Pamukkale University and Middle East Technical University Central Laboratory R&D Training and Measurement Center for FESEM, FTIR, and BET analysis.

Conflicts of Interest: The author declares no conflict of interest.

References

1. Khan, M. D.; Singh, A.; Khan, M. Z.; Tabraiz, S.; Sheikh, J. Current perspectives, recent advancements, and efficiencies of various dye-containing wastewater treatment technologies. *J. Water Process. Eng.* **2023**, *53*, 103579. https://doi.org/10.1016/j.jwpe.2023.103579.
2. Moradihamedani, P. Recent advances in dye removal from wastewater by membrane technology: a review. *Polym. Bull.* **2022**, *79*, 2603-2631. https://doi.org/10.1007/s00289-021-03603-2.
3. Gadekar, M. R.; Ahammed, M. M. Coagulation/flocculation process for dye removal using water treatment residuals: modelling through artificial neural networks. *Desalination Water Treat.* **2016**, *57*, 26392-26400. https://doi.org/10.1080/19443994.2016.1165150.
4. Constantin, M.; Asmarandei, I.; Harabagiu, V.; Ghimici, L.; Ascenzi, P.; Fundueanu, G. Removal of anionic dyes from aqueous solutions by an ion-exchanger based on pullulan microspheres. *Carbohydr. Polym.* **2013**, *91*, 74-84. https://doi.org/10.1016/j.carbpol.2012.08.005.
5. Ikhlaq, A.; Zafar, M.; Javed, F.; Yasar, A.; Akram, A.; Shabbir, S.; Qi, F. Catalytic ozonation for the removal of reactive black 5 (RB-5) dye using zeolites modified with $CuMn_2O_4/gC_3N_4$ in a synergic electro flocculation-catalytic ozonation process. *Water Sci. Technol.* **2021**, *84*, 1943-1953. https://doi.org/10.2166/wst.2021.404.
6. Vimonses, V.; Lei, S.; Jin, B.; Chow, C. W.; Saint, C. Adsorption of congo red by three Australian kaolins. *Appl. Clay Sci.* **2009**, *43*, 465-472. https://doi.org/10.1016/j.clay.2008.11.008.
7. Zheng, Y.; Cheng, B.; Fan, J.; Yu, J.; Ho, W. Review on nickel-based adsorption materials for Congo red. *J. Hazard. Mater.* **2021**, *403*, 123559. https://doi.org/10.1016/j.jhazmat.2020.123559.
8. Ausavasukhi, A.; Kampoosaen, C.; Kengnok, O. Adsorption characteristics of Congo red on carbonized leonardite. *J. Clean. Prod.* **2016**, *134*, 506-514. https://doi.org/10.1016/j.jclepro.2015.10.034.
9. Zhao, S.; Li, Y.; Wang, M.; Chen, B.; Zhang, Y.; Sun, Y.; Chen, K.; Du, Q.; Jing, Z.; Jin, Y. Preparation of MIL-88A micro/nanocrystals with different morphologies in different solvents for efficient removal of Congo red from water: Synthesis, characterization, and adsorption mechanisms. *Microporous Mesoporous Mater.* **2022**, *345*, 112241. https://doi.org/10.1016/j.micromeso.2022.112241.
10. Wang, X.; Xu, Q.; Zhang, L.; Pei, L.; Xue, H.; Li, Z. Adsorption of methylene blue and Congo red from aqueous solution on 3D MXene/carbon foam hybrid aerogels: A study by experimental and statistical physics modeling. *J. Environ. Chem. Eng.* **2023**, *11*, 109206. https://doi.org/10.1016/j.jece.2022.109206.
11. Onizuka, T.; Iwasaki, T. Low-temperature solvent-free synthesis of polycrystalline hematite nanoparticles via mechanochemical activation and their adsorption properties for Congo red. *Solid State Sci.* **2022**, *129*, 106917. https://doi.org/10.1016/j.solidstatesciences.2022.106917.

Preprints (www.preprints.org) | NOT PEER-REVIEWED | Posted: 12 July 2023 doi:10.20944/preprints202307.0755.v1

12. Kavitha, D.; Namasivayam, C. Recycling coir pith, an agricultural solid waste, for the removal of procion orange from wastewater. *Dyes Pigm.* **2007**, *74*, 237-248. https://doi.org/10.1016/j.dyepig.2006.01.040.
13. Gupta, N.; Kushwaha, A. K.; Chattopadhyaya, M. C. Application of potato (*Solanum tuberosum*) plant wastes for the removal of methylene blue and malachite green dye from aqueous solution. *Arab. J. Chem.* **2016**, *9*, S707-S716. https://doi.org/10.1016/j.arabjc.2011.07.021.
14. Sudrajat, H.; Susanti, A.; Putri, D. K. Y.; Hartuti, S. Mechanistic insights into the adsorption of methylene blue by particulate durian peel waste in water. *Water Sci. Technol.* **2021**, *84*, 1774-1792. https://doi.org/10.2166/wst.2021.361.
15. Sun, H.; Wang, X.; Wang, R.; Zhang, Y.; Wang, X. Biosorption of Cd^{2+} from aqueous solution by Ca^{2+}/Mg^{2+} type Citrus paradisi Macf. peel biosorbents. *Water Sci. Technol.* **2019**, *80*, 1205-1212. https://doi.org/10.2166/wst.2019.369.
16. Eldeeb, T. M.; Aigbe, U. O.; Ukhurebor, K. E.; Onyancha, R. B.; El-Nemr, M. A.; Hassaan, M. A.; Osibote, O. A.; Ragab, S.; Okundaye, B.; Balogun, V. A.; El Nemr, A. Biosorption of acid brown 14 dye to mandarin-CO-TETA derived from mandarin peels. *Biomass Convers. Biorefin.* **2022**, 1-21. https://doi.org/10.1007/s13399-022-02664-1.
17. Shakoor, S.; Nasar, A. Removal of methylene blue dye from artificially contaminated water using citrus limetta peel waste as a very low cost adsorbent. *J. Taiwan Inst. Chem. Eng.* **2016**, *66*, 154-163. https://doi.org/10.1016/j.jtice.2016.06.009.
18. Altunkaynak, Y.; Canpolat, M.; Yavuz, Ö. Adsorption of cobalt (II) ions from aqueous solution using orange peel waste: equilibrium, kinetic and thermodynamic studies. *J. Iran. Chem. Soc.* **2022**, *19*, 2437-2448. https://doi.org/10.1007/s13738-021-02458-8.
19. Gubitosa, J.; Rizzi, V.; Cignolo, D.; Fini, P.; Fanelli, F.; Cosma, P. From agricultural wastes to a resource: Kiwi Peels, as long-lasting, recyclable adsorbent, to remove emerging pollutants from water. The case of Ciprofloxacin removal. *Sustain. Chem. Pharm.* **2022**, *29*, 100749. https://doi.org/10.1016/j.scp.2022.100749.
20. Cho, E. J.; Lee, Y. G.; Chang, J.; Bae, H. J. A high-yield process for production of biosugars and hesperidin from mandarin peel wastes. *Molecules* **2020**, *25*, 4286. https://doi.org/10.3390/molecules25184286.
21. Jang, S. K.; Jung, C. D.; Seong, H.; Myung, S.; Kim, H. An integrated biorefinery process for mandarin peel waste elimination. *J. Clean. Prod.* **2022**, *371*, 133594. https://doi.org/10.1016/j.jclepro.2022.133594.
22. Bhatti, H. N.; Zaman, Q.; Kausar, A.; Noreen, S.; Iqbal, M. Efficient remediation of Zr (IV) using citrus peel waste biomass: Kinetic, equilibrium and thermodynamic studies. *Ecol. Eng.* **2016**, *95*, 216-228. https://doi.org/10.1016/j.ecoleng.2016.06.087.
23. Sadiq, A. C.; Olasupo, A.; Ngah, W. S. W.; Rahim, N. Y.; Suah, F. B. M. A decade development in the application of chitosan-based materials for dye adsorption: A short review. *Int. J. Biol. Macromol.* **2021**, *191*, 1151-1163. https://doi.org/10.1016/j.ijbiomac.2021.09.179.
24. Barus, D. A.; Humaidi, S.; Ginting, R. T.; Sitepu, J. Enhanced adsorption performance of chitosan/cellulose nanofiber isolated from durian peel waste/graphene oxide nanocomposite hydrogels. *Environ. Nanotechnol. Monit. Manag.* **2022**, *17*, 100650. https://doi.org/10.1016/j.enmm.2022.100650.
25. Habiba, U.; Siddique, T. A.; Joo, T. C.; Salleh, A.; Ang, B. C.; Afifi, A. M. Synthesis of chitosan/polyvinyl alcohol/zeolite composite for removal of methyl orange, Congo red and chromium (VI) by flocculation/adsorption. *Carbohydr. Polym.* **2017**, *157*, 1568-1576. https://doi.org/10.1016/j.carbpol.2016.11.037.
26. Abdić, Š.; Memić, M.; Šabanović, E.; Sulejmanović, J.; Begić, S. Adsorptive removal of eight heavy metals from aqueous solution by unmodified and modified agricultural waste: tangerine peel. *Int. J. Environ. Sci. Technol.* **2018**, *15*, 2511-2518. https://doi.org/10.1007/s13762-018-1645-7.
27. Pavithra, S.; Thandapani, G.; Sugashini, S.; Sudha, P. N.; Alkhamis, H. H.; Alrefaei, A. F.; Almutairi, M. H. Batch adsorption studies on surface tailored chitosan/orange peel hydrogel composite for the removal of Cr (VI) and Cu (II) ions from synthetic wastewater. *Chemosphere* **2021**, *271*, 129415. https://doi.org/10.1016/j.chemosphere.2020.129415.
28. Li, B.; Shan, C. L.; Zhou, Q.; Fang, Y.; Wang, Y. L.; Xu, F.; Han, L. R.; Ibrahim, M.; Guo, L. B.; Xie, G. L.; Sun, G. C. Synthesis, characterization, and antibacterial activity of cross-linked chitosan-glutaraldehyde. *Mar. Drugs* **2013**, *11*, 1534-1552. https://doi.org/10.3390/md11051534.
29. Ghorai, S.; Sarkar, A. K.; Panda, A. B.; Pal, S. Effective removal of Congo red dye from aqueous solution using modified xanthan gum/silica hybrid nanocomposite as adsorbent. *Bioresour. Technol.* **2013**, *144*, 485-491.

Preprints (www.preprints.org) | NOT PEER-REVIEWED | Posted: 12 July 2023 doi:10.20944/preprints202307.0755.v1

30. Lagergren, S. Zur theorie der sogenannten adsorption geloster stoffe, Kungliga Svenska Vetenskapsakademiens. *Handlingar* **1898**, *24*, 1-39.
31. Ho, Y. S.; McKay, G. Pseudo-second order model for sorption processes. *Process Biochem.* **1999**, *34*, 451-465. https://doi.org/10.1016/S0032-9592(98)00112-5.
32. Weber, W. J.; Morris, J. C. Advances in water pollution research: removal of biologically resistant pollutant from wastewater by adsorption. Proceedings of the Intern. Conf. on Water Pollution Symposium, 2, Pergamon Press, Oxford, UK, **1962**; 231-266.
33. Xie, B.; Qin, J.; Wang, S.; Li, X.; Sun, H.; Chen, W. Adsorption of phenol on commercial activated carbons: modelling and interpretation. *Int. J. Environ. Res. Public Health* **2020**, *17*, 789. https://doi.org/10.3390/ijerph17030789
34. Wang, B. E.; Hu, Y. Y.; Xie, L.; Peng, K. Biosorption behavior of azo dye by inactive CMC immobilized Aspergillus fumigatus beads. *Bioresour. Technol.* **2008**, *99*, 794-800. https://doi.org/10.1016/j.biortech.2007.01.043.
35. Zhang, H.; Ma, J.; Wang, F.; Chu, Y.; Yang, L.; Xia, M. Mechanism of carboxymethyl chitosan hybrid montmorillonite and adsorption of Pb (II) and Congo red by CMC-MMT organic-inorganic hybrid composite. *Int. J. Biol. Macromol.* **2020**, *149*, 1161-1169. https://doi.org/10.1016/j.ijbiomac.2020.01.201.
36. Ohemeng-Boahen, G.; Sewu, D. D.; Tran, H. N.; Woo, S. H. Enhanced adsorption of congo red from aqueous solution using chitosan/hematite nanocomposite hydrogel capsule fabricated via anionic surfactant gelation. *Colloids Surf. A: Physicochem. Eng. Asp.* **2021**, *625*, 126911. https://doi.org/10.1016/j.colsurfa.2021.126911.
37. Alardhi, S. M.; Fiyadh, S. S.; Salman, A. D.; Adelikhah, M. Prediction of methyl orange dye (MO) adsorption using activated carbon with an artificial neural network optimization modeling. *Heliyon* **2023**, *9*, e12888. https://doi.org/10.1016/j.heliyon.2023.e12888.
38. Langmuir, I. The adsorption of gases on plane surfaces of glass, mica and platinum. *J. Am. Chem. Soc.* **1918**, *40*, 1361–1403. https://doi.org/10.1021/ja02242a004.
39. Freundlich, H. M. F. Over the adsorption in solution. *J. Phys. Chem.* **1906**, *57*, 1100–1107.
40. Freundlich, H.; Heller, W. The adsorption of cis- and trans-azobenzene. *J. Am. Chem. Soc.* **1939**, *61*, 2228–2230. https://doi.org/10.1021/ja01877a071.
41. Pursell, C. J.; Hartshorn, H.; Ward, T.; Chandler, B. D.; Boccuzzi, F. Application of the Temkin model to the adsorption of CO on gold. *J. Phys. Chem. C* **2011**, *115*, 23880-23892. https://doi.org/10.1021/jp207103z.
42. Dubinin, M. The potential theory of adsorption of gases and vapors for adsorbents with energetically nonuniform surfaces. *Chem. Rev.* **1960**, *60*, 235-241. https://doi.org/10.1021/cr60204a006.
43. Mate, C. J.; Mishra, S. Synthesis of borax cross-linked Jhingan gum hydrogel for remediation of Remazol Brilliant Blue R (RBBR) dye from water: Adsorption isotherm, kinetic, thermodynamic and biodegradation studies. *Int. J. Biol. Macromol.* **2020**, *151*, 677-690. https://doi.org/10.1016/j.ijbiomac.2020.02.192.
44. Atkins, P.; de Paula, J.; Keeler, J. *Atkins' Physical Chemistry*, OUP Oxford, Oxford, **2017**.
45. Al-Harby, N. F.; Albahly, E. F.; Mohamed, N. A. Kinetics, isotherm and thermodynamic studies for efficient adsorption of Congo Red dye from aqueous solution onto novel cyanoguanidine-modified chitosan adsorbent. *Polymers* **2021**, *13*, 4446. https://doi.org/10.3390/polym13244446.
46. Wekoye, J. N.; Wanyonyi, W. C.; Wangila, P. T.; Tonui, M. K. Kinetic and equilibrium studies of Congo red dye adsorption on cabbage waste powder. *Environ. Toxicol. Chem.* **2020**, *2*, 24-31. https://doi.org/10.1016/j.enceco.2020.01.004.
47. Namasivayam, C.; Kavitha, D. Removal of Congo Red from water by adsorption onto activated carbon prepared from coir pith, an agricultural solid waste. *Dyes Pigm.* **2002**, *54*, 47-58. https://doi.org/10.1016/S0143-7208(02)00025-6
48. Sivarama Krishna, L.; Sreenath Reddy, A.; Muralikrishna, A.; Wan Zuhairi, W. Y.; Osman, H.; Varada Reddy, A. Utilization of the agricultural waste (Cicer arientinum Linn fruit shell biomass) as biosorbent for decolorization of Congo red. *Desalination Water Treat.* **2015**, *56*, 2181-2192. https://doi.org/10.1080/19443994.2014.958540.
49. Zhang, L.; Tu, L. Y.; Liang, Y.; Chen, Q.; Li, Z. S.; Li, C. H.; Wang, Z.H.; Li, W. Coconut-based activated carbon fibers for efficient adsorption of various organic dyes. *RSC Adv.* **2018**, *8*, 42280-42291. https://doi.org/10.1039/C8RA08990F.

Preprints (www.preprints.org) | NOT PEER-REVIEWED | Posted: 12 July 2023 doi:10.20944/preprints202307.0755.v1

50. Wang, Y.; Chen, R.; Dai, Z.; Yu, Q.; Miao, Y.; Xu, R. Facile preparation of a polypyrrole modified Chinese yam peel-based adsorbent: characterization, performance, and application in removal of Congo red dye. *RSC Adv.* **2022**, *12*, 9424-9434. https://doi.org/10.1039/d1ra08280a.
51. Dbik, A.; Bentahar, S.; El Khomri, M.; El Messaoudi, N.; Lacherai, A. Adsorption of Congo red dye from aqueous solutions using tunics of the corm of the saffron. *Mater. Today: Proc.* **2020**, *22*, 134-139. https://doi.org/10.1016/j.matpr.2019.08.148

Disclaimer/Publisher's Note: The statements, opinions and data contained in all publications are solely those of the individual author(s) and contributor(s) and not of MDPI and/or the editor(s). MDPI and/or the editor(s) disclaim responsibility for any injury to people or property resulting from any ideas, methods, instructions or products referred to in the content.